Renata SULIMA

ANALYSIS OF DYNAMIC MODEL OF STEC-TYPE MICROACTUATOR

ABSTRACT *The paper presents an analysis of the model of an electrostatic microactuator of comb-drive design. The analysis includes problems of strength and motion dynamics of the actuator. Calculations were performed for two designs of the moving comb electrode as well as an analysis of the drive's behavior at different power supply conditions. Dimensions of the individual suspension component parts were chosen and the shapes of the MEMS microactuator operating parts were verified.*

Keywords: *electrostatic microactuator, MEMS, dynamic analysis, mathematical simulation*

1. INTRODUCTION

The MEMS electrostatic microstructures can be divided into the flat and the comb-drive ones. The latter ones are divided into linear 14 and rotary 15. Many of the latter ones are described in the literature.

Renata SULIMA, M.Sc.
e-mail: r.sulima@iel.waw.pl

Electrotechnical Institute,
Pożaryskiego 28, 04-703 Warszawa, POLAND

PROCEEDINGS OF ELECTROTECHNICAL INSTITUTE, Issue 240, 2009

J.Berger, Y. Hang et al. 10 describe a comb drive for controlling a laser diode. That actuator can be rotated by an angle of ± 1.4° at a voltage of 140 V. Other solution is suggested by W. Piyawattanametha, P. R. Patterson et al. 11. It is a vertical comb-drive with an initial rotation of the comb fingers which permits to achieve a scanning angle of ± 4° at significantly lower voltage of 40V where the moving comb is assembled manually. The electrodes are set at a given angle and then blocked by a polisilicone latch. The solution of Xie H., Pan Y., Fedder G. K 12 is similar where the moving comb is made by DRIE etching. The natural process of arising residual stresses is used there to obtain the suitable angle of finger rotation in a thin metal layer deposited on the SCS substrate. At the same dimensions of the actuator system an angle of ± 4.7° was obtained at a voltage 18 V. An other concept was adopted by J. H. Lee, Y. C. Ko et al. 13 this actuator consist of two plates (of which the one is the scanning mirror) attached to the comb electrodes suspended on a torsional beam. This actuator controls a mirror, by 80% bigger then the other ones. A scanning angle of 12° was achieved in tests using dc voltage 28 V, or a sinusoidal voltage of 35 V 60 Hz.

Micromirrors with electrostatic actuation are often used in optical systems with displays, free space OXC (cross connects) for telecommunication nets and tomography 16.

The parameters required for such devices are quite stringent (high reliability, low insertion loss, low-polarization-dependent loss). Miniature MEMS systems using solid state technologies can satisfy these requirements , which insure small dimensions, high precision and reliability and low production cost if manufactured serially. MEMS system can perform single function as well as complicated multifunction tasks (lab-on-chip). In optical applications (ie optical switches) the switching time is very important. The optical signal is often converted into an electric signal, switched and again changed into an optical one. This process is complicated and time consuming resulting in slower data transfer in the wave guide network because of the so called “bottle neck” of the optical switch.

MEMS switches with micromirrors permit to switch signals directly from input to output which saves unnecessary transformation and removes the “bottle neck” effect and accelerates the whole network. An optical switch with micromirror is based solely on precise positioning of the mirror using an actuator, e.g. an electrostatic one. An important element is the proper selection of the control signal so that the control unit – the mirror, rotates by the required angle with the lowest possibly oscillations.

Reports made by EnablingMNT 4 and Nexus 5 show how high the demand for microstructures is. From them it can be seen that the highest demand is for RW heads (read/write) which doublet their turnover during the last 4 years.

Equally dynamic but with lower turnover are the markets of ink printer heads, microdisplay and pressure sensors. The markets of telecommunication MEMS can also be counted to strong development trends which has trebled its turnover since 2004 4.

2. DESIGNING THE STRUCTURE

The microswitch consists of two comb-electrodes in STEC configuration Fig. 1. A single comb consists of several, up to some hundreds rectangular plates (or of other shape) Fig. 2. When no voltage is applied, the elastic beam to which the plates are fixed, keeps them above the electrodes of the lower comb attached to the base.

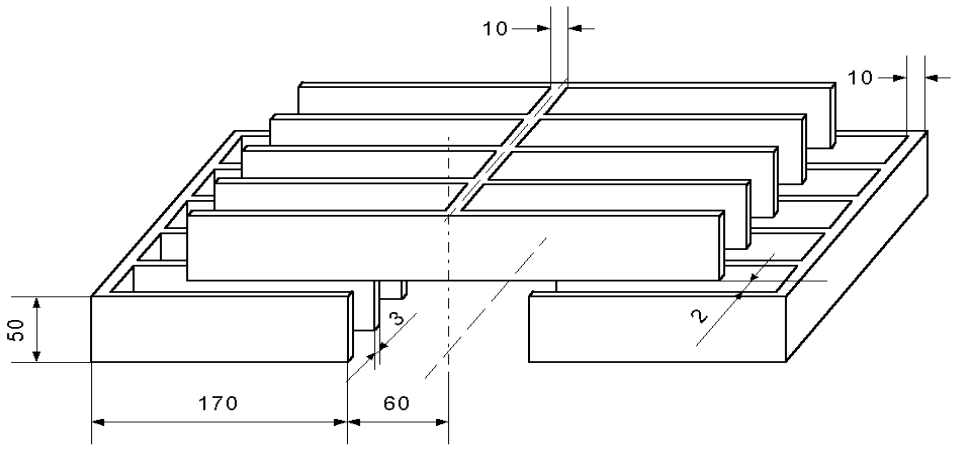

Fig. 1. Comb-drive microactuator in voltageless state

A. Electrostatic Model

In this case the moving electrode consists of 100 platelets. Its rotation angle is α = ±10°.

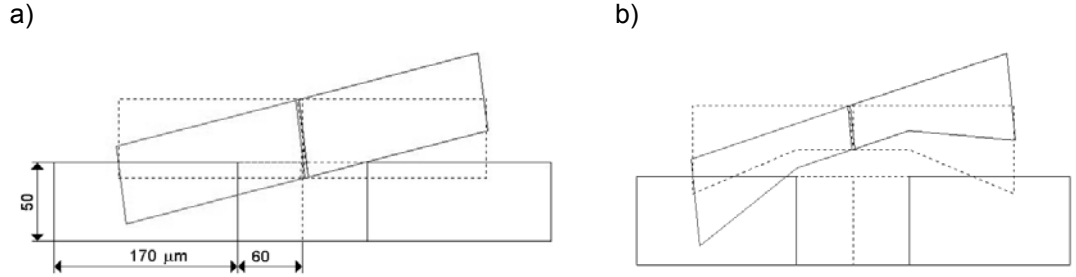

Fig. 2. Comb microactuator,
a) with rectangular fingers, b) with triangular fingers, after rotation

The network model 3, 6 presents the mathematical representation of the phenomena occurring in the electrostatic structure. The basic capacitance depends only on the active surface area of the co-operating electrodes, because the electrodes do not distance themselves from each other during operation according to the following relationship:

$$C_S = \frac{\varepsilon \cdot S}{d} = \frac{\varepsilon}{d} \sum S(\alpha) \tag{1}$$

where:

ε – the electrostatic constant of environment – air,
S – active surface area of the electrode,
d – distance between electrodes.

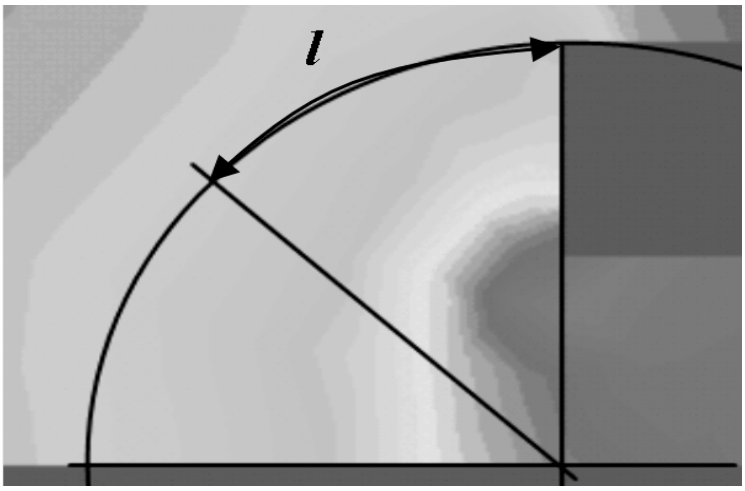

Fig. 3. The path covered by a charge moved from one electrode to the other one. The hypothetical equipotential surface gives through the symmetry axis of the cylinder segment formed by the field lines

The other component of the system's total capacitance is the stray capacitance at the electrode edges:

$$C_{rl} = \frac{q}{V} = \frac{4\varepsilon}{\pi \ln\left(\frac{d + h}{d}\right)} l_e(\alpha) \tag{2}$$

where:

q – the charge collected at the electrode surface,
h – thickness of a single electrode plate,
d – distance between electrodes,
l_e – active length of the cooperating electrode edges.

The third component of the total capacitance is the capacitance between the faces of the co-operating electrodes.

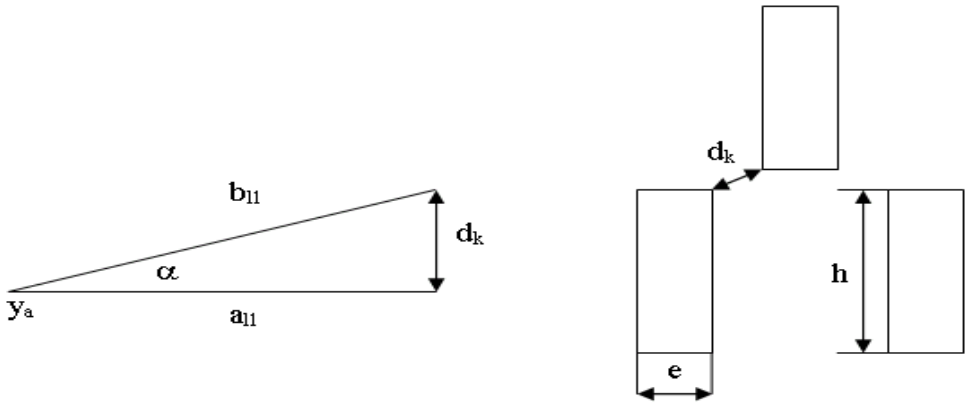

Fig. 4. Symbols adopted to determinate the stray capacitance at the faces of electrodes

The first relationship represents the capacitance of an elementary capacitor corresponding to the stray capacitance:

$$\Delta C_k = \frac{\varepsilon \cdot e}{4} \frac{\Delta b_{l1}}{\Delta d_k + \left(y_a - h\right)} \tag{3}$$

where:

e – electrode thickness,
Δb_{l1} – active length of the lower edges of the moving electrode,
Δd_k – distance electrode-to-electrode,
y_a – intersection point of moving electrode edge and the stationary electrode edge,
h – electrode height.

The stray capacitance at electrode faces is:

$$C_k = \sum_{j=1}^{n} C_{kj} \tag{4}$$

The total capacitance of the comb-drive system is the sum of the three component capacitances:

$$C_{tot} = C_S + C_{rl} + C_k \tag{5}$$

B. Determining the Electrostatic Force

Energy in an electrostatic system is described by the relationship:

$$W = \frac{1}{2} CU^2 = \frac{1}{2} U^2 \frac{\varepsilon}{d} S(\alpha) \tag{6}$$

where:

U – voltage applied to the capacitor,
C – capacitor capacity,
ε – dielectric permeability,
d – air gap.

In order to calculate the electrostatic force produced by the actuator, the partial derivative of energy by the y and α variables must be determined. The result is shown below. The force in direction y:

$$F_y = \frac{\partial W}{\partial y} = \frac{\varepsilon \cdot U^2}{2d} \frac{\partial S(\alpha)}{\partial y} \tag{7}$$

The torque determined for α:

$$M_\alpha = \frac{\partial W}{\partial \alpha} = \frac{\varepsilon \cdot U^2}{2d} \frac{\partial S(\alpha)}{\partial \alpha} \tag{8}$$

The moving electrode is placed on elastic beams which are exposed to torsion and to bending (as a result of carrying the weight of electrode plates).

C. Mechanical Model

The electrostatic actuator being analyzed here is made by micromachining polisilicone 3. The stationary comb electrode is placed on a silicone substrate and the moving electrode is suspended above it on an elastic beam.

In static problems the loading is produced volume forces, i.e. the weight of material. In a model the situation can be presented as a load distributed continuously along the whole length of a torsioned beam.

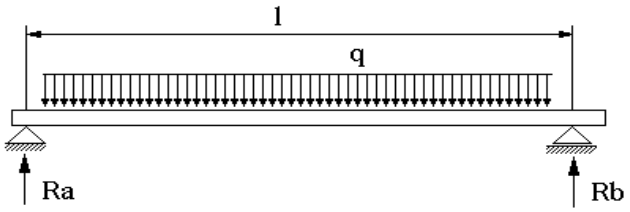

Fig. 5. Model of a bending load on a suspension beam

The bending moment:

$$M_g = R_A x - \int_0^x q(x-\zeta)d\zeta = \frac{ql}{2}x - \frac{qx^2}{2} \tag{9}$$

The max value of the bending moment at the point $x = \frac{l}{2}$:

$$M_{g\max\left(x=\frac{l}{2}\right)} = \frac{ql^2}{8} \tag{10}$$

The equation of the bent axis in differential form is presents below 7 :

$$\frac{M_g}{EI} = \pm \frac{y''}{\sqrt{\left[1+\left(y'\right)^2\right]^3}} \tag{11}$$

After simplifying:

$$\frac{d^2y}{dx^2} = \pm \frac{M_g}{EI} \tag{12}$$

After transformation and substituting, the bending moment:

$$EI\frac{d^2y}{dx^2} = M_{gA} = \frac{ql}{2}x \tag{13}$$

After integration we obtain:

$$EI\frac{dy}{dx}=\int_0^x\frac{ql}{2}xdx=\frac{ql}{4}x^2+C_1 \tag{14}$$

After the next integration we obtain:

$$EIy=\int_0^x\left(\frac{ql}{4}x^2+C_1\right)dx=\frac{ql}{4}\frac{x^3}{3}+C_1x+C_2 \tag{15}$$

The bending angle of the beam at the point of support A is:

$$\vartheta_A=\left(\frac{dy}{dx}\right)=\frac{1}{EI}\left(\frac{ql}{4}x^2+C_1\right) \tag{16}$$

The bending of the beam in the interval A is:

$$y=\frac{1}{EI}\left(\frac{ql}{12}x^3+C_1x+C_2\right) \tag{17}$$

The bending angle of the beam at the point of support B is:

$$\vartheta_B=\left(\frac{dy}{dx}\right)=\frac{1}{EI}\left(\frac{ql}{4}x^2-\frac{q}{6}x^3+C_3\right) \tag{18}$$

The bending of the beam in the interval B is:

$$y=\frac{1}{EI}\left(\frac{ql}{12}x^3-\frac{q}{24}x^4+C_3x+C_4\right) \tag{19}$$

D. Determining the Moments of Inertia

The polar inertia moment 8:

$$I_O=\int r^2dm=\int\left(x^2+y^2+z^2\right)dm=\frac{1}{2}\left(I_x+I_y+I_z\right) \tag{20}$$

The inertia moment with respect to axis z is:

$$I_z = I_O = I_x + I_y = \frac{m}{12}\left(h^2 + b^2\right) \tag{21}$$

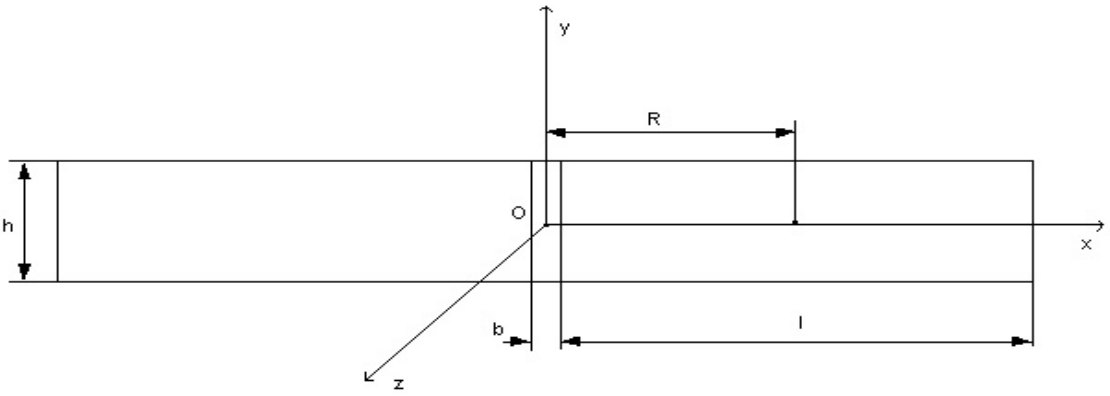

Fig. 6. Schematic diagram of calculating the moment of inertia of the moving comb

The moment of inertia of the beam versus axis z:

$$I_{zbel} = \frac{m_b}{12}\left(h^2 + b^2\right) \tag{22}$$

The moment of inertia of the finger versus axis z:

$$I_{zzeb} = I_{zzeb} + m_e\left(R\right)^2 = \frac{m_e}{12}\left(h^2 + 4l^2\right) \tag{23}$$

The moment of the inertia of whole finger-beam system is:

$$I_z = I_{zbel} + I_{zzeb} = \frac{m_b}{12}\left(h^2 + b^2\right) + \frac{m_e}{12}\left(h^2 + 4l^2\right) \tag{24}$$

E. Torsion of the Suspension Beam

Torsion of the suspension beam is caused by two forces: the force of weight of the electrodes fixed to the beam and by the electrostatic force.

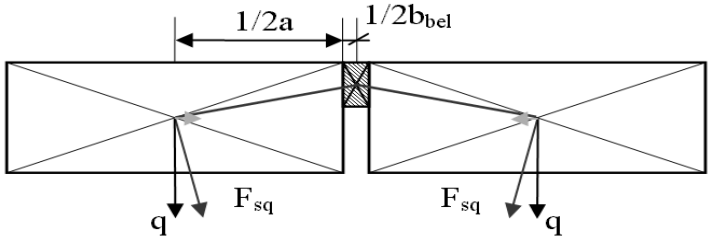

Fig. 7. Loading on the suspension beam by the electrodes torsion force F_{sq} acting on the beam originating from electrodes weight q

The centers of gravity of electrodes:

$$sc_x = \frac{1}{2} a_x = \frac{1}{n} \sum_{i=1}^{n} x_i \tag{25}$$

$$sc_y = \frac{1}{2} h_y = \frac{1}{n} \sum_{i=1}^{n} y_i \tag{26}$$

where:

h_y – the component y of electrode height.

The arm of action of the force originating from electrode weight:

$$r_{ce} = \sqrt{\left(\left(sc_x + \frac{1}{2} b_{bel} \right)^2 + sc_y^2 \right)} \tag{27}$$

Cosinus of the angle between the arm of force active and the electrode length:

$$\cos\gamma = \frac{\left(sc_x + \frac{1}{2} b_{bel} \right)}{r_{ce}} \tag{28}$$

The torsional moment from electrodes weight:

$$M_{sc} = r_{ce} \times F_{qs} = r_{ce} \cdot \frac{q}{\cos\gamma} \tag{29}$$

The resulting torsional moment is a sum of the moments originating from the electrostatic force and form the moment of electrode weight:

$$M_s = M_{sc} + M_{se} \tag{30}$$

Assuming that the system is ideally symmetric (the electrode weight at both beam sides is the same) the torsional moment from electrodes weight becomes zero and the resulting moment is equal to the moment from the electrostatic field.

As the angle of beam rotation is equal to the angle of beam torsion, the torsional moment can be expressed by the angle of beam torsion and the beam rigidity:

$$M_s = -GI_s\alpha \tag{31}$$

G – modulus of Kirchhoff.

Torsion strength index, where α – coefficient:

$$W_s = \alpha \cdot b^3 \tag{32}$$

Index to beam rigidity to torsion, where β – coefficient:

$$I_s = \beta \cdot b^4 \tag{33}$$

Max shearing stress in the suspension beam:

$$\tau_{\max} = \frac{M_s}{W_s} \tag{34}$$

Shearing stress in the middle of the shorter ends, where η – coefficient:

$$\tau^{'} = \eta\tau_{\max} \tag{35}$$

The rotation angle of the beam in degrees:

$$\theta = \frac{M_s}{G \cdot I_s}\frac{180}{\pi} \tag{36}$$

F. Calculation of the System's Kinetic Energy

The kinetic energy of a moving body equals half of the product of its mass multiplied by its velocity squared 8:

$$T = \frac{1}{2} m v^2 \tag{37}$$

where

m – mass of the body,
v – linear velocity.

In the case of a solid body rotating with the angular velocity ω around the axis z, the elementary point of a mass dm should be considered whose linear velocity is $v = \omega r$ where r is the distance of the point from the rotation axis. Its kinetic energy is:

$$\frac{1}{2} v^2 dm = \frac{1}{2} \omega^2 r^2 dm \tag{38}$$

Kinetic energy of a solid body is:

$$T = \frac{1}{2} \int v^2 dm = \frac{1}{2} \int \omega^2 r^2 dm = \frac{1}{2} \omega^2 \int r^2 dm \tag{39}$$

The expression under the integral $\int r^2 dm$ is equal to the moment of inertia with respect to the rotation axis, e.g. *Oz*. Substituting the corresponding moment of inertia it is possible to obtain a simpler relationship:

$$T = \frac{1}{2} I_z \omega^2 \tag{40}$$

The energy of external forces acting on electrodes can be written as a sum of all forces acting on the system:

$$L = \int_{\alpha_0}^{\alpha} M_s d\alpha \tag{41}$$

Considering the theorem on kinetic energy, the energy of forces rotating a body with the angularly velocity ω_0 at t_0 and ω at t we can write as:

$$\frac{1}{2} I_{zzeb} \omega^2 - \frac{1}{2} I_{zzeb} \omega_0^2 = L \tag{42}$$

It results from this that:

$$\frac{1}{2} I_{zzeb} \omega^2 - \frac{1}{2} I_{zzeb} \omega_0^2 = \int_{\alpha_0}^{\alpha} M_s d\alpha \tag{43}$$

Calculation of the integral in the area of the electrodes movement assuming an angle $\alpha = 0$ at the initial moment:

$$L = \int_{\alpha_0}^{\alpha} M_s d\alpha = \int_{\alpha_0}^{\alpha} \left(-GI_s\right) \alpha d\alpha = \left(-GI_s\right) \frac{\alpha^2}{2} \tag{44}$$

The angular velocity can be found comparing the kinetic energy with the energy of the external forces:

$$\frac{1}{2} I_{zzeb} \omega^2 = \left(-GI_s\right) \frac{\alpha^2}{2} \tag{45}$$

The angular rotation velocity of the moving comb of electrodes is:

$$\omega = \sqrt{\left(-GI_S\right) \frac{\alpha^2}{I_{zzeb}}} \tag{46}$$

G. The Natural Vibrations of the Electromechanical System

The rotation angle of the electrodes must satisfy the dynamic equation of the rotation movement. The dynamic equation of the rotational movement of the actuator comb is as below, concerning the relationship (34):

$$I_{zzeb} \ddot{\alpha} = M_s = -GI_S \alpha \tag{47}$$

We introduce the following notation:

$$k^2 = \frac{GI_s}{I_{zzeb}} \tag{48}$$

After substituting into the dynamic equation of motion we obtain:

$$\ddot{\alpha} + k^2 \alpha = 0 \tag{49}$$

When analyzing this equation it can be found that the electrodes will vibrate harmonically with the pulsation k whose period amounts to:

$$\tau = \frac{2\pi}{k} = 2\pi\sqrt{\frac{I_{zzeb}}{GI_S}} \tag{50}$$

The above characteristic presents the undamped vibrations of the comb-drive electrostatic actuator STEC.

H. Energy Model of the STEC Comb Microactuator

The mechanical co-energy of the moving comb electrode is 9:

$$E_k^{'}(\omega) = \frac{1}{2} I_{zzeb} \omega^2 \tag{51}$$

The co-energy of the electric field is:

$$E_e^{'}(U, \alpha) = \frac{1}{2} C(\alpha) U^2 \tag{52}$$

The total energy of the field basing on the Lagrange equation is 9:

$$E_c(\alpha, \phi) = E_p(\alpha) + W_m(\phi, \alpha) \tag{53}$$

where

ϕ – electric flux,

α – rotation angle.

In this case there is no effect of energy storing, so the potential energy of the system contains only the elastic element of the moving comb suspension.

$$E_c(\alpha,\phi) = E_p(\alpha) = \frac{\alpha^2}{2k} \tag{54}$$

where:

$k = GI_S$ – the constant of the elastic beam.

After this substitution the Lagrange function is expressed by the formula:

$$L(\omega,\alpha,U) = \frac{1}{2} I_{zzeb}\omega^2 + \frac{1}{2} C(\alpha)U^2 - \frac{\alpha^2}{2k} \tag{55}$$

In the system analyzed, the Rayleigh function is expressed by the formula:

$$R(\omega,U) = \frac{1}{2} D\omega^2 + \frac{1}{2} GU^2 \tag{56}$$

The only external force in this system is the source of electric power supply so the Lagrange equation for the mechanical part of the system has the form 9:

$$\frac{d}{dt}\left[\frac{\partial L(\omega,\alpha,U)}{\partial \omega}\right] - \frac{\partial L(\omega,\alpha,U)}{\partial \alpha} + \frac{R(\omega,U)}{\partial \omega} = F_{zew} \tag{57}$$

The following expressions are determined from the Lagrange and Rayleigh functions:

$$\frac{\partial L(\omega,\alpha,U)}{\partial \omega} = I_{zzeb}\omega \tag{58}$$

$$\frac{d}{dt}\left[\frac{\partial L(\omega,\alpha,U)}{\partial \omega}\right] = I_{zzeb}\frac{d^2\alpha}{dt^2} \tag{59}$$

and:

$$\frac{\partial L(\omega,\alpha,U)}{\partial \alpha} = \frac{1}{2} C(\alpha)U^2 - \frac{\alpha}{k} \tag{60}$$

The dissipation in this case is the torque of viscous friction:

$$\frac{R(\omega,U)}{\partial\omega} = D\omega \tag{61}$$

The dynamic equilibrium equation for the comb system is:

$$I_{zzeb}\frac{d^2\alpha}{dt^2} + D\omega + \frac{\alpha}{k} - \frac{1}{2}C(\alpha)U^2 = 0 \tag{62}$$

where:

$D = S\eta$ – viscous friction of the moving element in the environment (air),

S – surface area of the moving element suffering viscous friction,

η – viscous friction coefficient (for air $0.18\left[\frac{kg}{m\cdot s}\right]$).

3. CALCULATIONS RESULTS

A simulation model was built shown in Fig. 8. The voltage forcing applied to the moving electrodes of the actuator is a rectangular function with

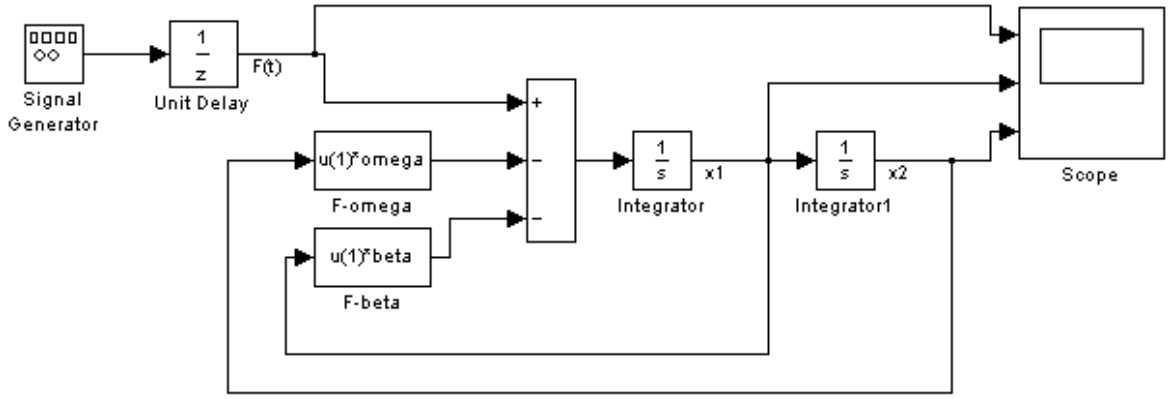

Fig. 8. The simulation model build in Simulink

a frequency of 0.9 kHz and amplitude equal to the torque produced at a single electrode. A block of delay was introduced in order to make the characteristic better visible. The symbols presented in Fig. 8 denote respectively:

$$\text{beta} = \frac{\text{coefficient of viscous damping}}{\text{polar moment of inertia of a finger}}$$

$$\text{omega} = \frac{\text{torque of the beam}}{\text{polar moment of inertia of a finger}}$$

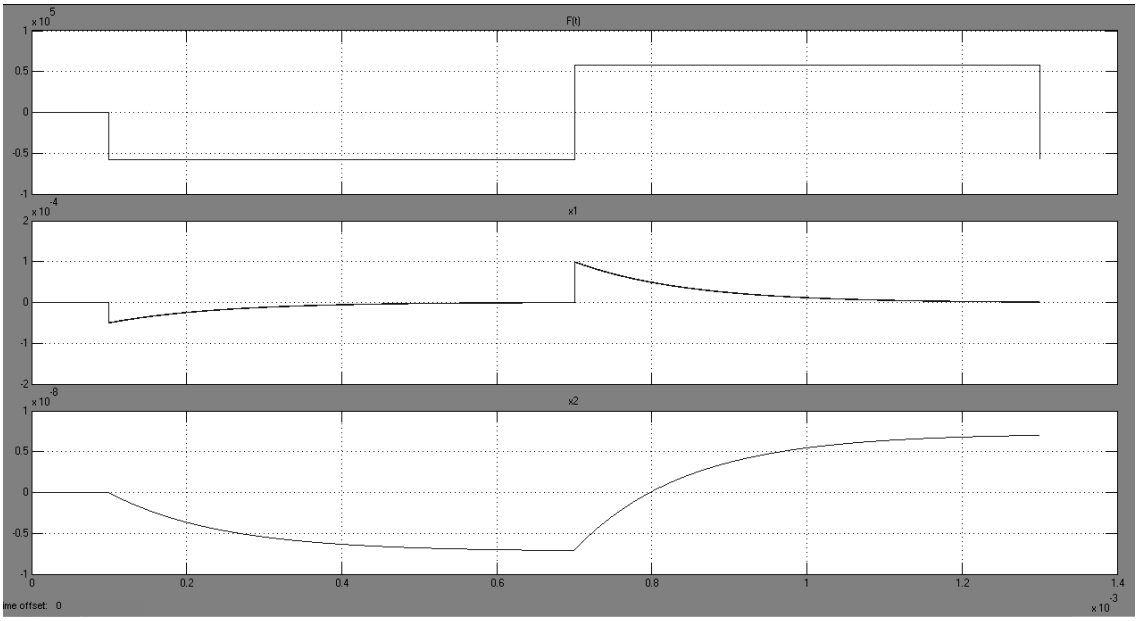

Fig. 9. The characteristics made in Matlab Simulink

Response of the system described by the differential equation of the second order is shown in Fig. 9. The first diagram represents the input signal, the second one –the angular velocity of the moving finger, the third one –the angular acceleration.

From the calculations made in Simulink it results that the system comes to the equilibrium state after switching, in a time 0.3 ms.

The analyzed system deflects by an angle ± 10° at applying a voltage amplitude 40 V.

4. CONCLUSION

The electrostatic comb microactuator STEC type was analyzed. The simulation was conducted for supply voltage amplitude of 40 V. From the

assumed comb dimensions a rotation angle of ± 10° of the moving structure was obtained. Input signal applied to the moving comb had a square waveform. The output characteristic of the system has the form of an inertial element with the transition time to equilibrium of 0.3 ms.

LITERATURE

1. Kazama A., Itou Y. et.al., *Low-Insertion-Loss Optical Matrix Switch Using MEMS Micromirrors Assembled by Passive Alignment*, JSME International Journal, Series B, Vol. 47, No. 3, 2004.
2. Patterson P.R., Hah D., et.al. *A Scanning Micromirror With Angular Comb Drive Actuation*, Fifteenth IEEE International Conference on Micro Electro Mechanical Systems, Las Vegas, 2002
3. Sulima R., *Modelling electrostatic microactuators used for driving scanning mirrors*, Engineering Mechanics, Vol. 12, No A1, pp 301-308, 2005.
4. MEMS Market Research: http://www.enablingMNT.com
5. MEMS Market Research: http://www.nexus-mems.com/usersupplier/mindetail.asp?ID=23
6. Sulima R., Wiak S., *Modelling of vertical electrostatic comb-drive for scanning micromirrors*, COMPEL, Vol. 27 no 4, 2008, pp 780-787
7. Dyląg Z., Jakubowicz A., Orłoś Z.: *Wytrzymałość materiałów* tom 1, Wydawnictwa Naukowo-Techniczne Warszawa 1996 (in Polish)
8. Leyko J.: *Mechanika ogólna* tom 2, Państwowe Wydawnictwa Naukowe, Warszawa 1978 (in Polish)
9. Meisel J.: *Zasady elektromechanicznego przetwarzania energii* , WNT Warszawa 1970. (in Polish)
10. J. D. Berger, Y. Zhang, et al.: *Widely tunable external cavity diode laser based on a MEMS electrostatic rotary actuator*, IEEE Optical Fiber Communication Conference and Exhibit, OFC 2001, Vol. 2, pp TuJ2-1-TuJ2-3
11. W. Piyawattanametha, P.R. Patterson, D. Hah, H. Toshiyoshi, M. C. Wu: *A surface and bulk micromachined angular vertical combdrive for scanning micromirrors*, IEEE Optical Fiber Communication Conference, OFC 2003, Vol. 1, pp 251-253
12. Xie H., Pan Y., Fedder G. K.: *A CMOS-MEMS mirror with curled-hinge comb drives*, Journal of Microelectromechanical Systems, vol.12, no.4, August 2003 pp. 450-457
13. J. H. Lee, Y. C. Ko, H. M. Jeong, B. S. Choi et al.: *SOI-based fabrication processes of the scanning mirror having vertical comb fingers*, Sensors and Actuators A 102, (2002), pp 11-18
14. Li J., Zhang Q. X., Liu A. Q.: *Advanced fiber optical switches using deep RIE (DRIE) fabrication* , Sensors and Actuators A 102 (2003) pp. 286-295.
15. Patterson P. R., Hah D., et al: *A scanning micromirror with angular comb drive actuation*, Oral-presented at the Fifteenth IEEE International Conference on Micro Electro Mechanical Systems (MEMS 2002), Las Vegas, Nevada, USA, January 20-24, 2002 pp. 544-547

16. Zhang J., Zhang Z., Lee Y. C., Bright V. M., Neff J.: *Design and investigation of multi-level digitally positioned micromirror for open-loop controlled applications*, Sensors and Actuators A 103 (2003) pp. 271-283

Manuscript submitted 09.02.2009
Reviewed by Jarosław Zadrożny

ANALIZA MODELU DYNAMICZNEGO AKTUATORA TYPU STEC

R. SULIMA

STRESZCZENIE *W artykule przeprowadzono analizę dynamiczną mikroprzełącznika elektrostatycznego opartego o model STEC (Staggered Torsional Electrostatic Combdrive). Konstrukcja przełącznika przedstawiona jest na rysunku 1. Mikroprzełącznik elektrostatyczny o budowie grzebieniowej składa się z dwóch zestawów płaskich prostokątnych lub o innym kształcie elektrod (rys. 2). Jeden z zestawów jest przytwierdzony do podłoża natomiast drugi zawieszony na elastycznej beleczce spełniającej rolę sprężyny, która to pomaga ruchomemu grzebieniowi w krótkim czasie osiągnąć stan równowagi.*

Na rysunkach 3 i 4 przedstawione zostały elementarne składowe pojemności całkowitej układu elektrostatycznego o ruchu obrotowym.

Model mechaniczny obejmuje obliczenia zginania beleczki zawieszenia pod wpływem ciężaru elektrod, skręcania beleczki pod wpływem ciężaru układu ruchomego oraz skręcania beleczki zawieszenia powstającego od momentu elektrostatycznego wytwarzanego pomiędzy płytkami grzebienia ruchomego i nieruchomego po przyłożeniu napięcia sterującego.

Zależność (62) przedstawia równanie dynamiczne elektrody ruchomej, które uwzględnia kształt elektrody oraz współczynnik tłumienia wiskotycznego poruszających się w szczelinach powietrznych płytek krzemowych.

Wykonano również obliczenia symulacyjne w pakiecie Simulink Matlab układu o elektrodach prostokątnych. Schemat blokowy przedstawiono na Fig. 8 *natomiast wyniki obliczeń znajdują się na rysunku 9.*

Z obliczeń wynika, że układ taki zasilany sygnałem napięciowym o amplitudzie napięcia 40 V może skręcać się o kąt ±10°. Przełącznik osiąga stan równowagi po czasie równym 0.3 ms.